

Prospectivity mapping of Iron oxide-Copper-Gold (IOCG) deposits using support vector machine method in Feyzaabad area (east of Iran)

Farzaneh Zandiyyeh^{1*}, Mohammad Reza Shayestefar¹, Hojat Ranjbar¹ and Saied Saadat²

¹Shahid Bahonar University of Kerman, Kerman, Iran

²Department of Geology, Mashhad Branch, Islamic Azad University, Mashhad, Iran

*Corresponding author's email: zandifar62me@yahoo.com

Abstract

Feyzaabad area is situated in the northeastern part of Iran that hosts mainly Iron Oxide Copper-Gold (IOCG) mineralization. In the present study, support vector machine (SVM), as a supervised classification method in mineral prospectivity mapping, is applied in 1:100000 Feyzaabad area, in east of Iran. Different evidential layers such as hydrothermal alteration, geological and geochemical data were integrated to generate prospectivity model for IOCG mineralization. The outcomes of the SVM method show that prospective target areas for IOCG deposits are defined mainly by vicinity to NE-SW trending faults and pyroclastic rocks (mainly tuff) and Au-Cu geochemical anomalies. These outcomes show that SVM is a potentially effective method in order to integrate multiple information evidence layers in predictive mapping of mineral prospectivity. The final prospectivity model investigation demonstrate that beside identifying known IOCG deposits, which were applied as training regions in the applied method to evaluate the SVM, the applied method has specified some new targets as well. So the target areas shown in the final prospectivity model can be applied for follow-up exploration of the IOCG deposits.

Keywords: Mineral prospectivity mapping, SVM method, IOCG, Feyzaabad.

1. Introduction

Mineral exploration is as a principal and complex process that the main aim is to explore new mineral potentials in a study area (Abedi et al., 2012). Different information layers of geosciences datasets consisting of geological data, geochemical data, geophysical data and remote sensing data (Carranza and Laborte, 2014) are integrated, analyzed and processed for mineral prospectivity mapping (MPM) to specify prospective regions. The computer and geographic information system (GIS) methods are able to visualize, process and analyze data (Zuo & Carranza, 2011).

Several approaches are applied for the MPM, which are classified as data-driven and knowledge-driven methods (Bonham-Carter, 1994; Carranza, 2008; Pan and Harris, 2000). Knowledge-driven methods for predicting of mineral prospectivity is suitable in regions which are less-explored (or so-called 'greenfields') geologically where no or very few known mineral deposits occurred (Lusty et al., 2012). In knowledge-driven methods for predicting of mineral prospectivity, the assigned weights to every spatial evidence

layer are based on geoscientist's knowledge. In contrast, it is suitable in regions which are moderately- to well-explored (or so-called 'brownfields'), where the main objective is to restrict new targets in order to explore undiscovered mineral deposits of the type sought (e.g., Mejía-Herrera et al., 2014), some examples of these methods are Boolean logic (Bonham-Carter et al., 1989), index overlay (Bonham-Carter et al., 1989), the Dempster-Shafer belief theory (Moon, 1990) and fuzzy logic (An et al., 1991; Chung and Moon, 1990). In data-driven methods, the assigned weights to every informative evidence layers are quantified spatial relationships between the known deposits and particular data sets applied to show prospectivity identification criteria (Carranza and Laborte, 2014). Data-driven predictive mapping of mineral prospectivity contain different methods such as weight of evidence (Bonham-Carter et al., 1989), logistic regression (Agterberg and Bonham-Carter, 1999), Neural networks (Porwal et al., 2003; Singer and Kousta, 1996), evidential belief functions (Carranza, 2008; Carranza and Hale, 2002) and Bayesian network classifiers (Porwal et al., 2006).

Indeed MPM as classification process is used in order to identify new prospective regions, if data of the previous exploration projects are accessible (Yousefi et al., 2012; Najafi et al., 2014). Classification can be classified as supervised and unsupervised classification. In supervised classification, the label of classes which require to be classified in to is known in advance. In contrast, unsupervised classification doesn't need the human foreknowledge of the classes; actually it is also known as clustering. The supervised classification is the crucial tool which is applied for extracting quantitative information. Using this method, the analyst access to enough known pixels to create representative parameters for each evidential layer. Unsupervised classification doesn't need the human precognition of the classes, and mostly it uses some clustering algorithm in order to categorize the evidential information layers.

Support vector machines (SVMs) are the supervised learning models which use the learning algorithms for analyzing data and identifying patterns, for classifying and regression analysis. It was suggested by Vapnik (1995) as a data-driven method. This method were used in different contexts, such as classification of land cover (Otukey and Blaschke, 2010; Paneque-Gálvez et al., 2013), flood susceptibility mapping and assessment (Shafapour Tehrany et al., 2014, 2015), mineral prospectivity mapping (Zuo and Carranza, 2011; Abedi et al., 2012; Rodriguez-Gallano et al., 2015), land slide susceptibility (Peng et al., 2014; Pradhan, 2013; Yao et al., 2008); hydraulic unit prediction (Ali et al., 2013) and lithological classification (Yu et al., 2012).

In order to illustrate the power of the SVM method in this study, we applied several evidential layers including hydrothermal alteration, geological and geochemical data to produce the Iron Oxide Copper-Gold (IOCG) mineralization prospectivity map in Feyzaabad area, east of Iran. At the end, the produced prospectivity model was assessed using the known mineral potentials as testing points. In this study, SVM is proved as a strong and efficient tool for integrating multiple evidential layers for mineral prospectivity mapping.

2. Data and methodology

2.1. The support vector machine (SVM) method

The original SVM algorithm as a supervised learning method was invented by Vapnik et al. (1963). Boser et al. (1992) presented a way to produce nonlinear classifiers by using the kernel trick for maximum-margin hyperplanes. The present standard type (soft margin) was suggested by Cortes and Vapnik in 1993 and published in 1995.

A Support Vector Machine (SVM) carries out classification by finding the hyperplane that maximizes the margin between the two classes. The hyperplane which is defined by the vectors (cases) are the support vectors (Vapnik et al., 1992). The SVM algorithm is included three steps: first define an optimal hyperplane for maximizing margin, second, expand the above definition for non-linearly separable problems in order to have a penalty term for misclassifications finally, data are mapped in high dimensional space where it is easier to classify with linear decision surfaces in other words reformulate problem so that data is mapped implicitly to this space.

The optimum separation hyperplane (OSH) is the linear classifier with the maximum margin for a given finite set of learning patterns. The OSH computation with a linear support vector machine is presented in this section.

For classifying of two classes of patterns that are separated linearly, i.e., a linear classifier can perfectly separate them (Fig. 1).

The linear classifier is the hyperplane H ($w \cdot x + b = 0$) with the maximum width (distance between hyperplanes H_1 and H_2). Consider a linear classifier characterized by the set of pairs (w, b) that satisfies the following inequalities for any pattern x_i in the training set: (William et al., 2007)

$$\begin{cases} w \cdot x_i + b > +1 & \text{if } y_i = +1 \\ w \cdot x_i + b < -1 & \text{if } y_i = -1 \end{cases} \quad (1)$$

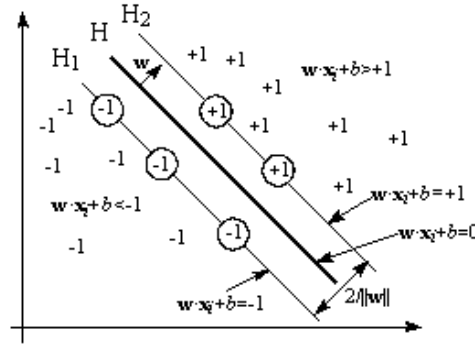


Fig.1. Hyperplane with maximum-margin and margins for an SVM trained with samples from two classes. Samples on the margin are called the support vectors(Kavzoglu and Colkesen, 2009).

The compact form of the equations can be expressed as:

$$y_i(w \cdot x_i + b) \geq +1$$

or

$$y_i(w \cdot x_i + b) - 1 \geq 0$$

Because we have studied the case of linearly separable classes, each such hyperplane (w, b) is a classifier which properly separates all patterns from the training set:

$$class(x_i) = \begin{cases} +1 & \text{if } w \cdot x_i + b > 0 \\ -1 & \text{if } w \cdot x_i + b < 0 \end{cases} \quad (2)$$

For all points from the hyperplane H ($w \cdot x + b = 0$), the distance between origin and the hyperplane H is $|b|/||w||$. We study the patterns from the class -1 that convince the equality $w \cdot x + b = -1$, and determine the hyperplane H_1 ; the distance between origin and the hyperplane H_1 is equal to $|-1-b|/||w||$. Similarly, the patterns from the class +1 convince the equality $w \cdot x + b = +1$, and determine the hyperplane H_2 ; the distance between origin and the hyperplane H_2 is equal to $|+1-b|/||w||$. Of course, hyperplanes H , H_1 and H_2 are parallel and no training patterns are located between hyperplanes H_1 and H_2 . Based on the above considerations, the distance between hyperplanes (margin) H_1 and H_2 is $2/||w||$.

From these considerations it follows that the identification of the optimum separation hyperplane is carried out by maximizing $2/||w||$, which is equivalent to minimizing $||w||^2/2$. finding the optimum separation hyperplane is a problem that is represented by the identification of (w, b) which convinces the equation (1) (Burgess, 1998).

The beauty of SVM is that if the data is linearly separable, there is a unique global minimum value. An ideal SVM analysis should generate a hyperplane that totally separates the vectors (cases) into two non-overlapping classes. However, perfect separation may not be possible, or it may result in a model with so many cases that the model does not classify correctly. In this case SVM finds the hyperplane that maximizes the margin and minimizes the misclassifications.

Separating two groups with a straight line is the simplest (1 dimension), flat plane (2 dimensions) or an N-dimensional hyperplane. However, there are cases where a nonlinear region can separate the groups more efficiently. SVM controls this by applying a kernel function (nonlinear) for mapping the data into a different space where a hyperplane (linear) cannot be applied to do the separation. It means a non-linear function is learned by a linear learning machine in a high-dimensional feature space while the capacity of the system is controlled by a parameter that does not depend on the dimensionality of the space. This is called kernel trick which means the kernel function transform the data into a higher dimensional feature space to make it possible to carry out the linear separation.

In 1992, Bernhard E. Boser, Isabelle M. Guyon and Vladimir N. Vapnik suggested a way to make nonlinear classifiers by using the kernel trick (originally proposed by Aizerman et al., 1964) to maximum-margin hyperplanes (Boser et al., 1992). The choice of a kernel function (K) and its parameters for an SVM are crucial for obtaining good results (Zuo and Carranza, 2011).

2.2. Spectral angle mapper (SAM)

Spectral angel mapper (SAM) is a spectral classification which applied an n-D angle to match pixels to reference spectra (Van der Meer et al., 1997; Crosta et al., 1998; Hunter and Power, 2002). The algorithm calculates the angle between two spectra which then determines the spectral similarity between them. This method was when applied on calibrated reflectance spectra, is relatively insensible to illumination and albedo effects (Crosta et al., 1998; Kruse et al., 1993). We can apply the SAM end member spectra used that can come from ASCII files, spectral libraries, or can be extracted directly from images (as ROI average spectra). This method measures the angle between the end member spectrum vector and each pixel vector in n-D space. Smaller angles show closer matches to the reference spectrum. Pixels further away than the nominative maximum angle threshold in radians are not classified (Kruse, 1988).

2.3. Logratio transformation

In order to eliminate the spurious relationships between compositions, the family of logratio-transformations is used to deal with the closure effects. In practice, these transformations are commonly used in geochemical data processing to open closed systems in order to understand the realistic relationships among compositions better (Carranza, 2011; Egozcue et al., 2003; Filzmoser et al., 2012; Wang et al., 2013). In this study, the data were then transformed using Isometric logratio (ilr). Isometric logratio (ilr) transformations are efficient category of logratio transformations with good theoretical

properties (Egozcue et al., 2003). For a D-part composition x , an ilr transformation can be selected as $z=(Z_1, \dots, Z_{D-1})=ilr(x)$ with:

$$z_i = \sqrt{\frac{D-i}{D-i+1}} \ln \frac{x_i}{\sqrt{\prod_{j=i+1}^D x_j}} \text{ for } i = 1, \dots, D-1$$

2.4. Data characteristics and pre-processing

In this study, five information layers were applied to make a prospectivity map. Table 1 describes the criteria, the informative evidence layers and the causes for applying them in the study.

For generating the faults and host rocks evidential layers related to the geological criteria, 1:100000 scale geological map of the study area was used. For alteration mapping, we used two ASTER scenes which were pre-processed up to Level 1B. These images were acquired on 18 June, 2007. These scenes were georeferenced using an orthorectified enhanced thematic mapper plus (ETM+) image in the UTM projection (zone 40) with the WGS-84 ellipsoid as a datum. The log-residual algorithm was used for atmospheric correction which decreases topography, instruments and sun illumination noises. The outcome of the log-residual algorithm is more representative of the soils types or lithologies of the areas in comparison with the raw data. Therefore, a spectrum resulted from data processed using the log-residual technique will be more nearly comparable to its related library spectrum. For the hydrothermal alteration mapping in the study area, the spectral angel mapper (SAM) was applied.

Table 1. Summary of evidential layers applied in the study.

| Criteria | Evidence layer | | cause of applying |
|--------------|--|--|--------------------------------------|
| Geology | Alteration | Argillic Propylitic Sericitic Silicic Iron oxide | Proper area for ore metal occurrence |
| | Faults Host rock | Pyroclastic rocks Heat Sources | |
| Geochemistry | Copper Anomaly (Cu) Gold Anomaly (Au) | | Ore-metal enrichment |

To produce an evidential map of geochemical signature (e.g, Carranza, 2008; Yousefi et al., 2014; Yousefi and Carranza, 2015), we applied stream sediment samples of Cu and Au data. In the study area, there is a data set for 1033 composite basic samples of -40 mesh (0.44 mm) fraction of stream sediments (collected by Exploration Co. Jiangxi on behalf of geological survey of Iran). The collected samples were analyzed for 28 elements. The concentration of Au and Cu elements in the samples were detected by Spectroscopy with chemical enrichment (Es-I) and coupled plasmas atomic emission spectroscopy (ICP) method (Exploration Co. Jiangxi, 1994) respectively. In stream sediment geochemical exploration, regardless of chemical pollution, the variation from the normal form has two syngenetic and epigenetic components; where the syngenetic component is related with petrogenesis and epigenetic component is related to economical mineralization that is known as the explorative useful component. Enrichment index is mainly independent of petrographic variations and

reduces the random errors. Therefore, generally it is used for the elimination of petrographical effects (Hasanipak and Sharafaldin, 2004). After calculating the enrichment index for different rock communities in Feyzaabad area, the resulted data of Au and Cu elements were integrated with each other and they were considered as one statistical community. Because stream sediment geochemical data set is an example of a closed number system, so an isometric logratio transformation (ilr) (Egozcue et al., 2003; Filzmoser et al., 2009) was directed to handle this problem.

2. Geology of the study area

The study area is situated in Taknar zone, which is uplifted in the form of a wedge block in north of Darouneh fault. The Taknar mineralization zone is underlain by Precambrian and Paleozoic basement, and overlain by Mesozoic and Cenozoic cover. There are facial and structural differences between this zone and adjacent zones (Fig. 2).

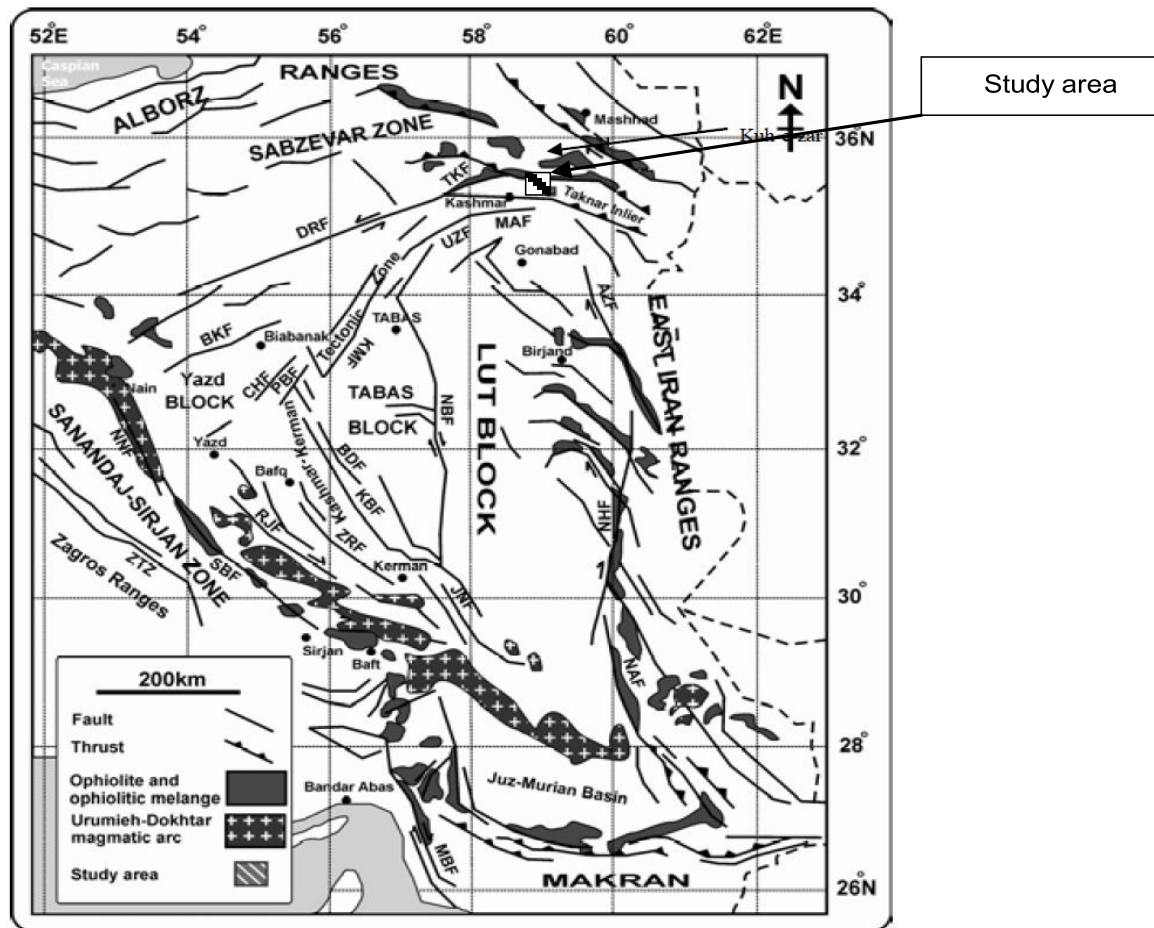


Fig.2. Tectonic map of the east of Iran (modified after Alavi, 1991 and Ramezani and Tucker, 2003).

This zone is limited by two main faults: Darouneh fault in the south and Rivash or Taknar fault in the north. Both faults are of slip-strike type and have an approximate east-west trend (Fig. 2). This zone is specified by vast exposure of volcanic and sub-volcanic rocks. several types of metal ore deposits, such as porphyry Cu, Cu-Au-Fe-oxide (IOCG), massive sulfide, Au-epithermal, intrusion-related gold systems and Sn-W skarn and also non-metal deposits like bentonite, kaolinite, etc. have been reported in the Taknar zone (Karimpour et al., 2009; Karimpour and Stern, 2009; Karimpour and Moradi, 2010; Malekzadeh et al., 2010; Abdi and Karimpour, 2013; Karimpour et al., 2014; Najafi et al., 2014).

Volcanic activities during Tertiary in east of the Taknar zone, between Darouneh and Taknar faults, start with dark grey tuffs, occasionally of ignimbrite type, accompanied with andesitic black lavas. On this unit, we can see a large thickness of white breccia tuffs, volcanic breccias, grey sandy tuffs, ignimbrites and lapilly tuffs. According to the 1:100,000 geological map of Feyzaabad (Heiydari, 2011) in the south of Hesar village, the conglomerates are overlain on the set of units with the same dip. To the east of Hesar village, there are sandstone, volcanic breccias, and sand tuffs with andesitic and trachy-andesitic lavas. In northeast of Alishir mountain, trachy-andesites are having porphyritic texture. The last product of the volcanic activities in this time period is pyroxene andesite, alkali basalt and trachy andesite in north of Khosh Darreh (east of study area). This set has porphyritic and glumero-porphyritic texture. in the aforesaid set, pyroxene and olivine minerals are found in the background which composed of plagioclases and alkali feldspars (Heiydari, 2011).

The Eocene facies in northeast of the study area, i.e. in Shast Darreh mountains is different with the other facies in the area, and it starts with light grey conglomerates involving limestone of Cretaceous age with occasionally andesites. This conglomerate unit is covered by thick green tuff interbedded with limestone and marl which are of Eocene age (Heiydari, 2011).

Two main types of copper, gold and iron-oxide mineralization like porphyry and vein

type have been reported from the study area (Karimpour et al., 2006; Mazloomi et al., 2008) (Fig.3).

4. IOCG deposits models

IOCG deposits involve many various ore systems and are found on all continents in general in Post-Archean rocks from the Early Proterozoic to the Pliocene (Hitzman, 2000). Host rocks in the neighborhood of ore bodies show severe hydrothermal alteration. In the close neighborhood of the ore, the variable pressure-temperature conditions of alteration and mineralization are reflected in a spectrum of deposits ranging from those in which the dominant Fe oxide is magnetite and alteration is specified by minerals such as biotite, K-feldspar and amphibole through to hematite dominated systems in which the main silicate alteration phases are sericite and chlorite. Economic mineralization is controlled by paragenetically late chalcopyrite \pm bornite and occurs within or near (but typically not coextensive with) Fe-oxide accumulations. Distal and shallow mineralization is hematite-dominated, whereas magnetite forms deeper and earlier. Metals not precipitated in these S-poor, moderately oxidized environments could potentially form distal halos (e.g., Zn-Pb, Mn, or Ag-Co-U). Individual mineralized centers seldom expand more than a few km across; yet mineralized regions can remain over regions 10s to 100s of km when defined by the intermittent distribution of magnetite- or hematite-rich rocks. Both local and regional mineralized zones correlate with main regional structural features (e.g., in coastal Chile, NW Queensland, northern Sweden) and/or with volcano-plutonic structures (e.g., in South Australia, northern Mexico, SE Missouri). Few districts have been thoroughly studied thus details of temporal and spatial patterns of alteration, magmatism (where present), and mineralization remain poorly constrained. In better mapped regions such as NW Queensland, coastal Chile, or the southwestern United States it is clear that multiple IOCG-like alteration episodes occurred intermittently over tens of millions of years. Only minorities of occurrences have economically interesting Cu-Au mineralization and that is typically interpreted to be late in the

regional development (Hitzman, 2000). For example, in NW Queensland, significant volumes of Na (Ca)-dominated rocks clearly represent multiple events; some of these are meta-evaporites and predate younger, metasomatic varieties that accompanied multiple styles of Fe-oxide \pm Cu(-Au) mineralization (Williams and Pollard, 2001). In individual districts, histories can be complicated and do not have simple patterns. There is an association with main fault systems that likely acted as brittle-ductile shear systems of transpressional to transtensional character at the time of granitoid intrusion and mineralization (Pollard, 2000). Comparison of larger and well-described IOCG deposits explains the geologic variety of the class as a whole. They occur in a wide range of different host rocks, among which plutonic granitoids, andesitic (meta) volcanic rocks, and (meta) siliclastic–metabasic rock associations are particularly important. Host rocks may be widely similar in age to the ore (e.g., Olympic Dam, Candelaria-Punta del Cobre, Raul Condestable) but in other cases significantly precede mineralization such that ore formation relates to a quite separate geologic event (e.g.,

Salobo, Ernest Henrt) (Williams et al., 2005). Major Cu-Au deposits of IOCG style are temporally associated with oxidized potassic granitoids similar to those linked to major porphyry Cu-Au deposits. Main copper-gold deposits in IOCG provinces range from diorite to syenogranite in composition (Pollard, 2000). Different genetic models have been suggested for IOCG deposits that can be widely divided in to those including magmatic and non-magmatic fluid sources (as summarized by Barton and Johnson, 2004). Magmatic models include the release of oxidized, sulfur-poor, metalliferous brines from the coeval magmas, with ore deposition subsequently driven by various processes. The sources are variously deduced to have been primitive calc-alkaline arc magmas. Non-magmatic models can be subdivided into two categories, the one in which fluids are mainly derived from the surface or shallow basins, and those including fluids that have developed in lower to midcrustal metamorphic environments (Williams et al., 2005). Because of a lack of important data that present important directions for future research the collective model is currently clouded in uncertainty.

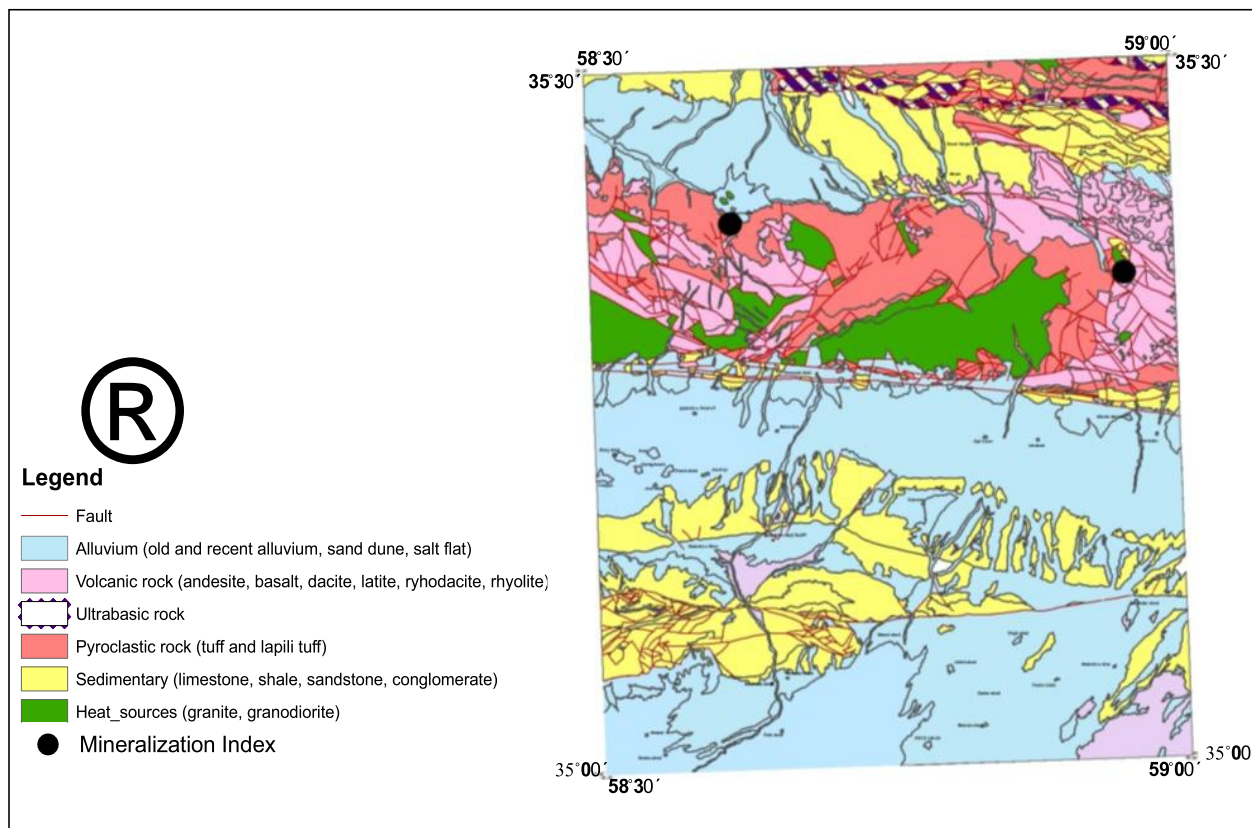


Fig.3. Simplified geological and mineral indexes map (1:100,000 scale) of the study area (Behrouzi, 1987).

5. Application of the SVM in Feyyzaabad region

5.1. Geo-exploration evidence layers for MPM

In this applied MPM approach for this study, the geo-exploration data are chose by using the data sets of the previous exploration projects and specification of IOCG deposits in the study area. We applied following geo-exploration evidential layers as the most important criteria for prospecting the IOCG deposits in the study area: lithology of the host rock, lithology of intrusive rocks as heat sources, proximity to the faults, alteration zones, and stream sediment geochemical anomaly of indicator elements.

In the current study, five information layers are applied to make a prospectivity map

(Table 1). For producing the geological evidence layers, classified maps of host rock lithology, heat sources and fault were extracted from the 1:100000 scale geological map of the study area. According to 1:100000 scale geological map of the study area and host rocks of known IOCG deposits in the study area, white tuff breccias, ignimbrite, green lapilli tuff, sandy tuff and granodiorites are favorable for IOCG mineralization, and were used in the integration process (Fig. 4a).

Spectral angle mapper (SAM) was performed on ASTER images of the study area to map zones of hydrothermal alteration and iron oxide/hydroxide minerals. Rocks which are located next to NE-SW faults are crushed and altered so they have maximum potential compared with no-fault areas (Fig.4b).

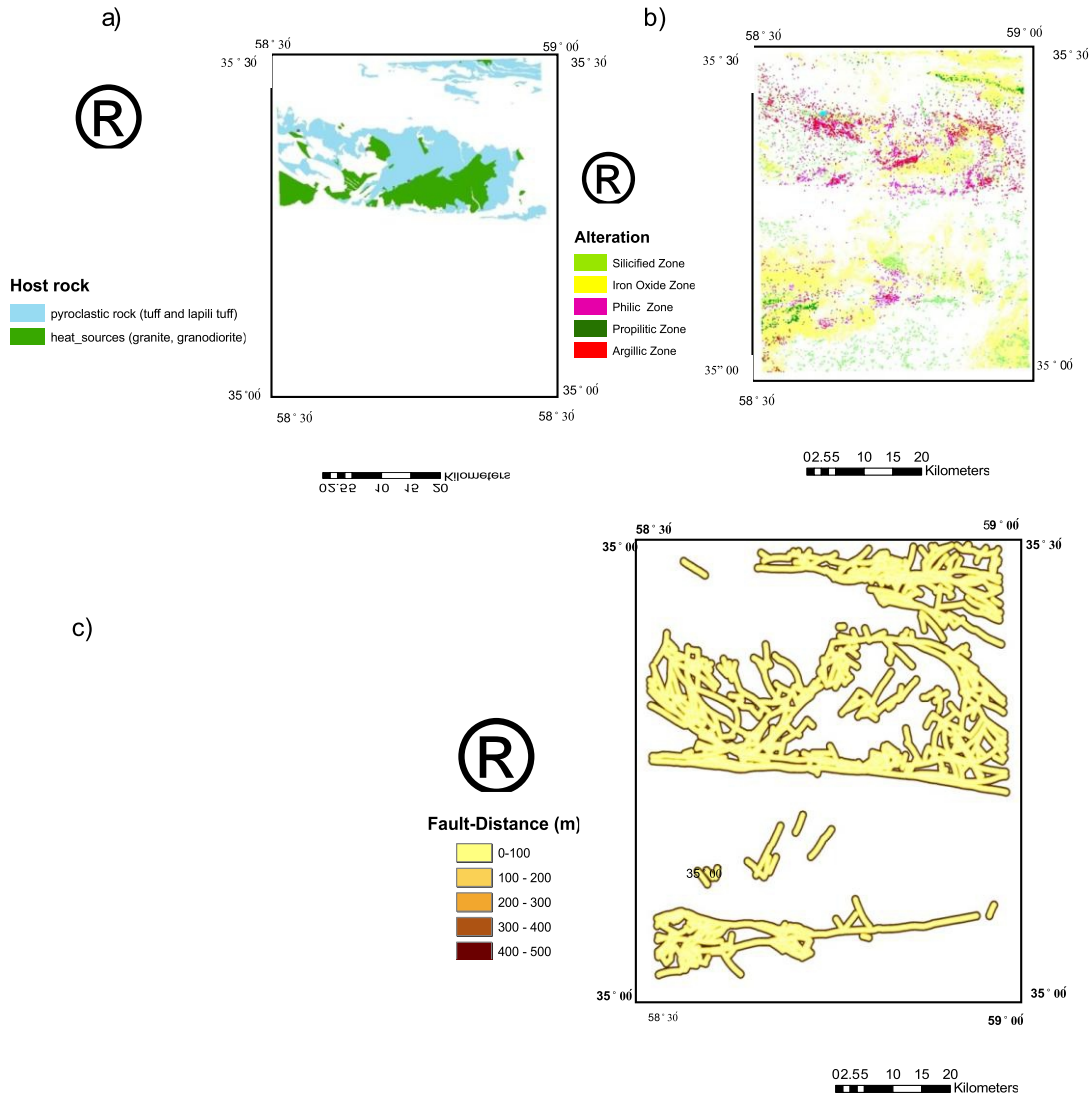


Fig.4. Geological evidential layers (a) host rock; (b) alteration zones (c) faults.

To generate evidential map of Au and Cu geochemical signature (e.g, Carranza, 2008; Yousefi et al., 2012, 2014; Yousefi and Carranza, 2015) we used stream sediment samples results, after removing the closure effect with ilr transformation. The geochemical data were interpolated by an inverse distance weighted (IDW) method in order to separate the concentration-area (C-A) and fractal analysis (Cheng et al., 1994, 1996, 1997, 2000) was adapted for separating background and anomalies. The maps of the Cu and Au geochemical distributions are shown in Fig.5. The analysis of the 1:250000 scale aeromagnetic data showed that the magnetic characteristics of the area did not show any correlation with the known mineralization. Therefore, this data was not used for MPM.

5.2 Application of the SVM

Five evidential layers were considered as main criteria in order to use the SVM method. Different regions of interest (ROI) were selected, which were used as feature vectors of the geosciences variables and a target variable for classification of mineral prospectivity (Table 1). The target feature vector is either the 'non-favorable' class (or 0) or the 'favorable' class (or 1) representing whether mineral exploration target is absent or present, respectively. For 'favorable' locations, we used

the four known IOCG deposits and some area with favorable conditions for IOCG deposits. For 'non-favorable' locations, we randomly selected them. Supervised SVM classification methodology was applied by sigmoid kernel with $\lambda = 0.25$ and $r = 0$. Algorithm that explains implementation of SVM is given below (Fan et al., 2008): First of all, loop the n data items and divide the input data set into two sets of data corresponding to two different categories, if a data item is not assigned any of the regions mentioned then add it to set of support vectors V .

The patterns of the predicted prospective target areas for IOCG deposits are defined mostly by neighboring to NE–SW trending faults, vicinity to pyroclastic rocks (mainly tuff) and Au geochemical anomaly (Fig. 6). The prospective target areas that are predicted, occupy 5% of the study area and contain 100% of the known IOCG deposits (Fig. 6).

4.3. Evaluation of the prospectivity model

The data integration outcome is a map showing the favorable area of IOCG deposits exploration (Fig. 6). Some percentages of favorable areas are located close to Tannurjeh (Karimpour et al., 2006) (Fig.7) and Kuh-e-Zar deposits (Mazloomi et al., 2008) (Fig. 8) as known mineral deposits.

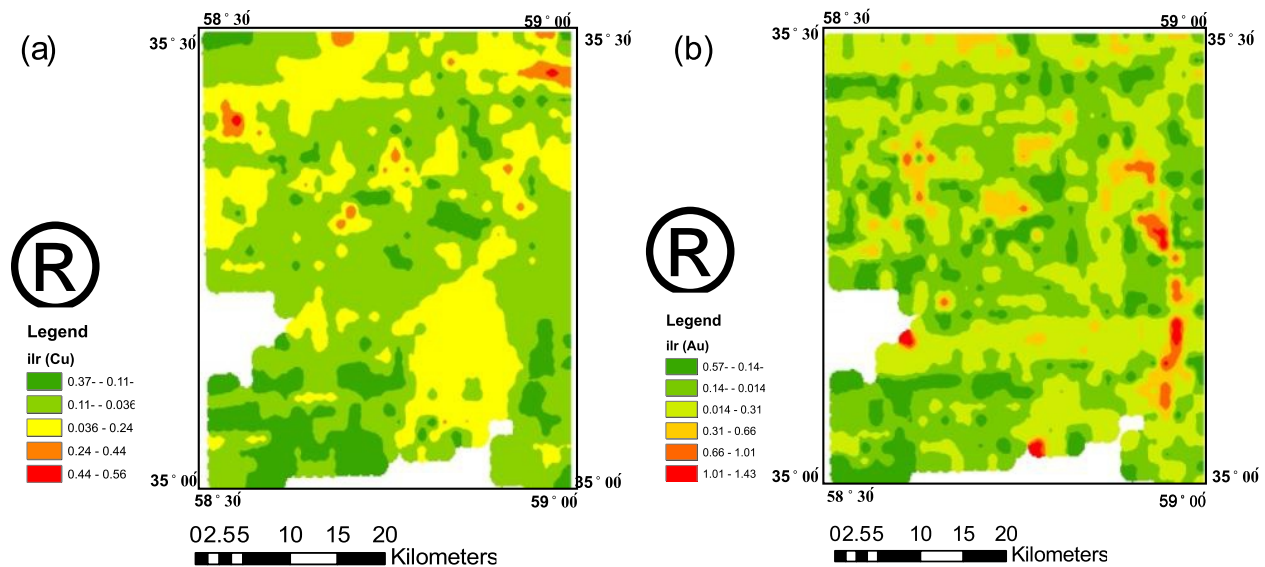


Fig. 5. Geochemical evidential layers: (a) Au; (b) Cu.

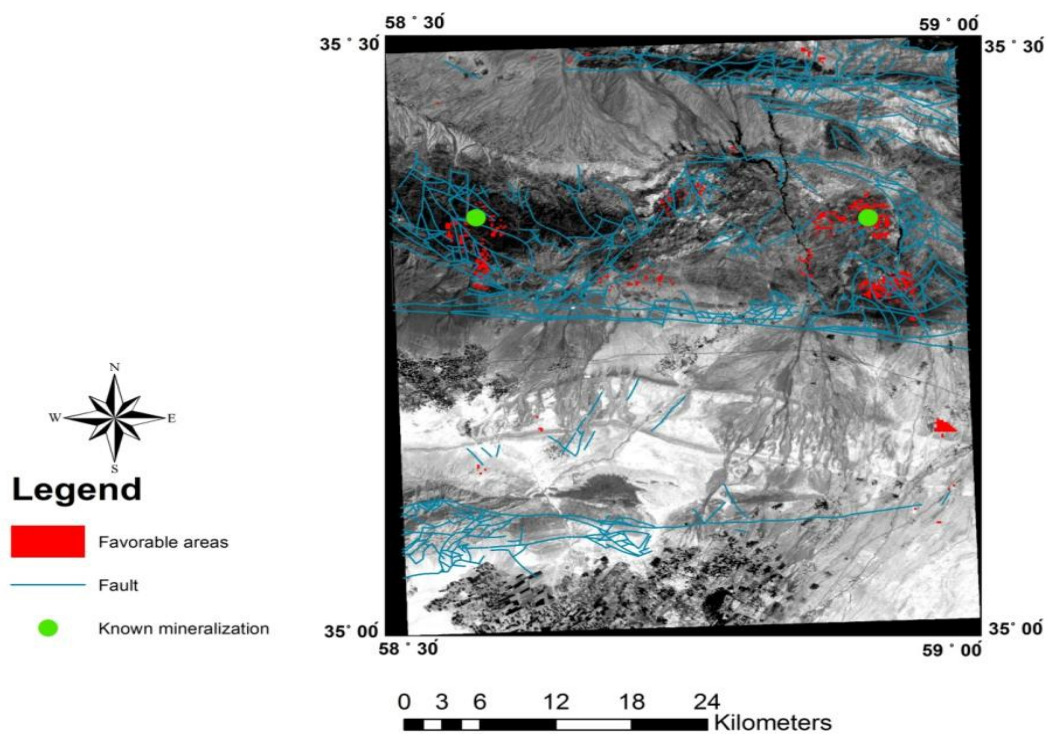


Fig. 6. Prospective targets area for IOCG deposits delineated by SVM.



Fig. 7. Tannurjeh IOCG deposit (a) Argillic and Argillic+Iron oxide alterations; (b) The quartz included gold (Au) as vein, veinlet and disseminated magnetite.

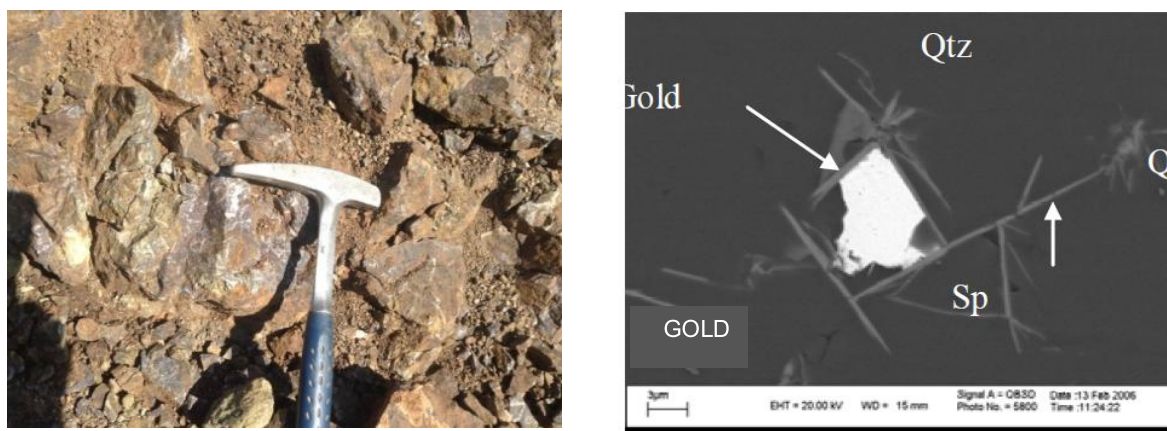


Fig. 8. (a): The quartz and specularite veins included gold (Au) mineralization; (b) Free gold (Au) particles surrounded with specularite.

6. Discussion and conclusion

In the current study, the support vector machine (SVM) was applied as a supervised method in data-driven mineral prospectivity mapping with integrating multiple variables to generate a prospectivity map in 1:100000 Feyzaabad area, in east of Iran.

The outcomes of the SVM method show that prospective target areas for IOCG deposits are defined mostly by neighboring to NE–SW trending faults and pyroclastic rocks (mainly tuff) and Au–Cu geochemical anomalies. These outcomes show that SVM is a potentially effective method in order to integrate multiple information evidence layers in mineral prospectivity mapping. Also applying this method results the reduction of the amount of risk for exploratory projects managers. The final prospectivity model investigation (Fig. 6) demonstrate that beside identifying known IOCG deposits, which were used as training regions in the applied method to assess the SVM, the applied method has specified some new targets as well. So the target areas produced in the final prospectivity model can be applied for follow-up exploration of the IOCG deposits.

References

- Abedi, M., Nourouzi, Gh., Bahroudi, A., 2012. Support vector machine for multi-classification of mineral prospectivity areas, *Computers & Geosciences*, 46, 272–283.
- Agterberg, F.P., Bonham-Carter, G.F., 1999. Logistic regression and weights of evidence modeling in mineral exploration. In: *Proceedings of the 28th International Symposium on Applications of Computer in the Mineral Industry (APCOM)*, Golden, Colorado, pp. 483–490.
- Aizerman, Mark A.; Braverman, Emmanuel M.; and Rozonoer, Lev I. 1964. Theoretical foundations of the potential function method in pattern recognition learning". *Automation and Remote Control*, 25, 821–837.
- Ali, S.S., Nizamuddin, S., Abdulraheem, A., Hassan, Md.R., Hossain, M.E., 2013. Hydraulic unit prediction using support vector machine, *Journal of Petroleum Science and Engineering*, 110, 243–252.
- An, P., Moon, W.M., Bonham-Carter, G.F., 1992. On knowledge-based approach on integrating remote sensing, geophysical and geological information. In: *Proceedings of International Geoscience and Remote Sensing Symposium (IGARSS)*, 1992, pp. 34–38.
- Barton, M.D., Johnson, D.A., 2004. Footprints of Fe-oxide (-Cu–Au) systems. SEG, 2004. *Predictive Mineral Discovery Under Cover*. Centre for Global Metallogeny, Spec. Pub. 33, The University of Western Australia, pp. 112–116.
- Bonham-Carter, G.F., 1994, *Geographic Information Systems for Geoscientists: Modelling with GIS*. Pergamon, Ontario, 398pp.
- Bonham-Carter, G.F., Agterberg, F.P., Wright, D.F., 1989. Weights of evidence modelling: a new approach to mapping mineral potential. In: Agterberg, F.P., Bonham-Carter, G.F. (Eds.), *Statistical Applications in the Earth Sciences*. Geological Survey of Canada, Paper 89-9, pp. 171–183.
- Boser, B. E.; Guyon, I. M.; Vapnik, V. N., 1992. A training algorithm for optimal margin classifiers. *Proceedings of the fifth annual workshop on Computational learning theory - COLT '92*. p. 144. doi:10.1145/130385.130401. ISBN 089791497X.
- Carranza, E.J.M., Hale, M., 2002. Wildcat mapping of gold potential, Baguio district, Philippines. *Transactions of the Institution of Mining and Metallurgy (Section B—Applied Earth Science)* 111, 100–105.
- Carranza, E.J.M., Laborte, A.G., 2014. Data-driven predictive mapping of gold prospectivity, Baguio district, Philippines: Application of Random Forests algorithm, *Ore Geology Reviews*, <http://dx.doi.org/10.1016/j.oregeorev.2014.08.010>.
- Carranza, E.J.M., 2008. Geochemical anomaly and mineral prospectivity mapping in GIS. In: *Handbook of Exploration and Environmental Geochemistry*, vol. 11, Elsevier, Amsterdam, 351 pp.

- Cortes, C., Vapnik, V., 1995. Support-vector networks, *Machine Learning*, 20(3), 273-297.
- Fan, R.E., Chang, K.W., Hsieh, C.J., Wang, X.R., Lin, C.J., 2008. LIBLINEAR: A library for large linear classification, *Journal of Machine Learning Research*, 9, 1871-1874.
- Heydari, A., 2011, Exploration report of Kuh Zar deposit in Torbat-e-Heydarieh area, Zarmehr mining company, 133p.
- Hitzman, M.W., 2000. Iron oxide-Cu-Au deposits: what, where, when, and why. In: Porter, T.M. (Ed.), *Hydrothermal Iron Oxide Copper-gold & Related Deposits: A Global Perspective*, vol. 2. PGC Publishing, Adelaide, Australia, pp. 9-25.
- Kavzoglu, T., Colkesen, I., 2009. A kernel functions analysis for support vector machines for land cover classification. *International Journal of Applied Earth Observation and Geoinformation* 11, 352-359.
- Lusty, P.A.J., Scheib, C., Gunn, A.G., Walker, A.S.D., 2012. Reconnaissance-scale prospectivity analysis for gold mineralisation in the southern Uplands-Down-Longford Terrane, Northern Ireland. *Nat. Resour. Res.* 21, 359-382.
- Macharis, C., Springael, J., Brucker, K.D., Verbeke, A., 2004. PROMETHEE and AHP: the design of operational synergies in multi criteria analysis. Strengthening PROMETHEE with ideas of AHP. *Eur. J. Oper. Res.* 153, 307-317.
- Mejía-Herrera, P., Royer, J.J., Caumon, G., Cheilletz, A., 2014. Curvature attribute from surface restoration as predictor variable in Kupferschiefer copper potentials. *Natural Resources, Res.* <http://dx.doi.org/10.1007/s11053-014-9247-7>.
- Moon, W.M., 1990. Integration of geophysical and geological data using evidential belief function. *IEEE Trans. Geosci. Remote Sens.* 28, 711-720.
- Najafi, A., Karimpour, M.H., Ghaderi, M., 2014. Application of fuzzy AHP method to IOCG prospectivity mapping: A case study in Taherabad prospecting area, eastern Iran, *International Journal of Applied Earth Observation and Geo information*, 33, 142-154.
- Otukei, J.R., Blaschke, T., 2010. Land cover change assessment using decision trees, support vector machines and maximum likelihood classification algorithms, *International Journal of Applied Earth Observation and Geoinformation*, 12(1), 527-531.
- Pan, G., Harris, D.P., 2000. *Information Synthesis for Mineral Exploration*. Oxford Univ. Press, New York, 461 pp.
- Peng, L., Niu, R., Huang, B., Wu, X., Zhao, Y., Ye, R., 2014. Landslide susceptibility mapping based on rough set theory and support vector machines: A case of the Three Gorges area, China, *Geomorphology*, 204, 287-301.
- Peng, X., Wang, Y., Xu, D., 2013. Structural twin parametric-margin support vector machine for binary classification, *Knowledge-Based Systems*, 49, I S S N 09507051, <http://dx.doi.org/10.1016/j.knsys.2013.04.013>, pages 6372.
- Pollard, P.J., 2000. Evidence of a magmatic fluid and metal source for Fe-oxide Cu-Au mineralisation. In: Porter, T.M. (Ed.), *Hydrothermal Iron Oxide Copper-Gold & Related Deposits: A Global Perspective*, vol. 1. Australian Mineral Foundation, Adelaide, Australia, pp. 27-46.
- Porwal, A., Carranza, E.J.M., Hale, M., 2003. Artificial neural networks for mineral-potential mapping: a case study from Aravalli Province, Western India. *Natural Resources Research*, 12, 156-171.
- Porwal, A., Carranza, E.J.M., Hale, M., 2006. A hybrid fuzzy weights-of-evidence model for mineral potential mapping. *Natural Resources Research*, 15, 1-14.
- Pradhan, B., 2013. A comparative study on the predictive ability of the decision tree, support vector machine and neuro-fuzzy models in landslide susceptibility mapping using GIS, *Computers & Geosciences*, 51, 350-365.
- Rao, T., Rajinikanth, T.V., Supervised Classification of Remote Sensed data Using Support Vector Machine, *Global Journal of Computer Science and Technology: Software & Data Engineering*, 14(1), 71-76.

- Rodriguez-Gallano, V., Sanchez-Castillo, M., Chica-Olmo, M., Chica-Rivas, M., 2015. Machine learning predictive models for mineral prospectivity, An evaluation of neural networks, random forest, regression trees and support vector machines, *Ore Geology Reviews*, doi:10.1016/j.oregeorev.2015.01.001.
- Shafapour Tehrany, M., Pradhan, B., Mansor, S., Ahmad, N., 2015. Flood susceptibility assessment using GIS-based support vector machine model with different kernel types, *CATENA*, 125, 91-101.
- Shafapour Tehrany, M., Pradhan, B., Neamah Jebur, M., 2014. Flood susceptibility mapping using a novel ensemble weights-of-evidence and support vector machine models in GIS, *Journal of Hydrology*, 512, 332-343.
- Singer, D.A., Kouda, R., 1996. Application of a feedforward neural network in the search for Kuruko deposits in the Hokuroku district, Japan. *Mathematical Geology*, 28, 1017-1023.
- Vapnik, V., 1995. *Nature of Statistical Learning Theory*. John Wiley and Sons, Inc., New York.
- Williams, P.J., Barton, M.D., Johnson, D.A., Fontbote, L., de Haller, A., Mark, G., Oliver, N.H.S., Marschik, R., 2005. Iron oxide copper gold deposits; geology, space-time distribution, and possible modes of origin. *Economic Geology*, 100, 371-406.
- William H.; Teukolsky, Saul A.; Vetterling, William T.; Flannery, B. P., 2007, Section 16.5. Support Vector Machines". *Numerical Recipes: The Art of Scientific Computing* (3rd ed.). New York: Cambridge University Press.
- Yao, X., Tham, L.G., Dai, F.C., 2008. Landslide susceptibility mapping based on Support Vector Machine: A case study on natural slopes of Hong Kong, China, *Geomorphology*, 101(4), 572-582.
- Yousefi, M., Carranza, E.J.M., 2015. Prediction-area (P-A) plot and C-A fractal analysis to classify and evaluate evidential maps for mineral prospectivity modeling, *Computers and Geosciences*, 79, 69-81.
- Yousefi, M., Kamkar-Rouhani, A., Carranza, E.J.M., 2012. Geochemical mineralization probability index (GMPI): a new approach to generate enhanced streamsediment geochemical evidential map for increasing probability of success in mineral potential mapping. *J. Geochem. Explor.* 115, 24-35.
- Yousefi, M., Kamkar-Rouhani, A., Carranza, E.J.M., 2014. Application of staged factor analysis and logistic function to create a fuzzy stream sediment geochemical evidence layer for mineral prospectivity mapping. *Geochem.: Explor. Environ. Anal.* 14, 45-58.
- Yu, L., Porwal, A., Holden, E.J., Dentith, M., 2012. Towards automatic lithological classification from remote sensing data using support vector machines, *Computers & Geosciences*, 45, 229-239.
- Zuo, R., Carranza, E.J.M., 2011. Support vector machine: A tool for mapping mineral prospectivity, *Computers & Geosciences*, 37, 1967-1975.